

TEMPORAL AND SPATIAL VARIABILITY OF HIGH RESOLUTION IN SITU VERTICAL APPARENT RESISTIVITY MEASUREMENTS AT A LNAPL IMPACTED SITE

D. Dale Werkema Jr.¹, Estella A. Atekwana², Anthony Endres³, and William A. Sauck¹

¹Dept. of Geosciences
Western Michigan University
Kalamazoo, MI 49008
dale@gsintl.net

²Dept. of Geology and Geophysics
University of Missouri-Rolla
Rolla, MO. 65409

³Environmental Geophysics Facility
Department of Earth Sciences
University of Waterloo
Waterloo, Ontario N2L 3G1
CANADA

Abstract

Ten high resolution vertical resistivity probes (VRPs) have been installed within plume and off plume locations at a LNAPL contaminated site adjacent to a former oil refinery in Carson City, MI. The VRPs are sealed PVC wells with stainless steel screws, serving as electrodes, spaced every 2 inches (5.08 cm) with depth. VRP measurements of apparent resistivity and monitoring well measurements of the water table were made monthly during a full calendar year. The apparent resistivity response from VRPs within the free product plume, within the residual plume, and at a clean non-contaminated location is compared. Further comparison of the temporal resistivity variation and water table fluctuations are also presented. The VRP results reveal that the natural hydrogeologic regime is not present in LNAPL contaminated areas as the fluctuating water table is not observed in these VRPs, but is evident in the non-contaminated VRP. Select VRP depth sections and depth slices indicate that the apparent resistivity is lowest at the LNAPL free product locations, progressively higher in the LNAPL dissolved location and highest in the clean (i.e. non-contaminated) location. These VRP sections also respond in like form to precipitation events, however at the contaminated locations the magnitude of change is greatly suppressed. A simple analysis using Archie's Law reveals that a large pore water saturation and a large pore water conductivity enhancement is necessary to produce the VRP field results from contaminated locations. We believe these results support our conductive model at LNAPL contaminated sites due to the effects of enhanced mineral dissolution of the aquifer materials resulting from biodegradation of the contaminant mass. Finally, the results demonstrate the potential for the use of vertical resistivity probes in understanding vadose zone processes and hydrogeologic dynamics at a LNAPL impacted site.

Introduction

This paper presents results from our continued study of the light non-aqueous phase liquid (LNAPL) plume present in the Carson City Park, Carson City Michigan. Previous work (Atekwana et. al, 2000, Sauck, 2000, Sauck et. al., 1998, Werkema et. al, 2000) have suggested the presence of anomalously low resistivity (high conductivity) coincident with areas of LNAPL contamination, contradicting previously acceptable geoelectric models of an insulating layer due to the presence of LNAPL contamination (DeRyck et. al., 1993). Furthermore, we have provided additional evidence of high oil degrading bacteria populations in zones coincident with the observed low apparent resistivity suggesting a possible link between the biodegradation of the LNAPL impacted zone and the geoelectrically low resistivities observed (Werkema et al., 2000, Cassidy et al., 2001). Finally, recent laboratory experiments provide further evidence suggesting that LNAPL biodegradation under aerobic

and anaerobic conditions can substantially change pore water biogeochemistry producing dramatic increases in conductivity (Cassidy et al., 2001).

In this study, we present the results of long term vertical apparent resistivity measurements from vertical resistivity probes (VRPs) installed in different subsurface contaminant conditions throughout the Carson City Park, MI. These results further test our conductive plume model of LNAPL contamination in glacially derived unconsolidated sand and gravel.

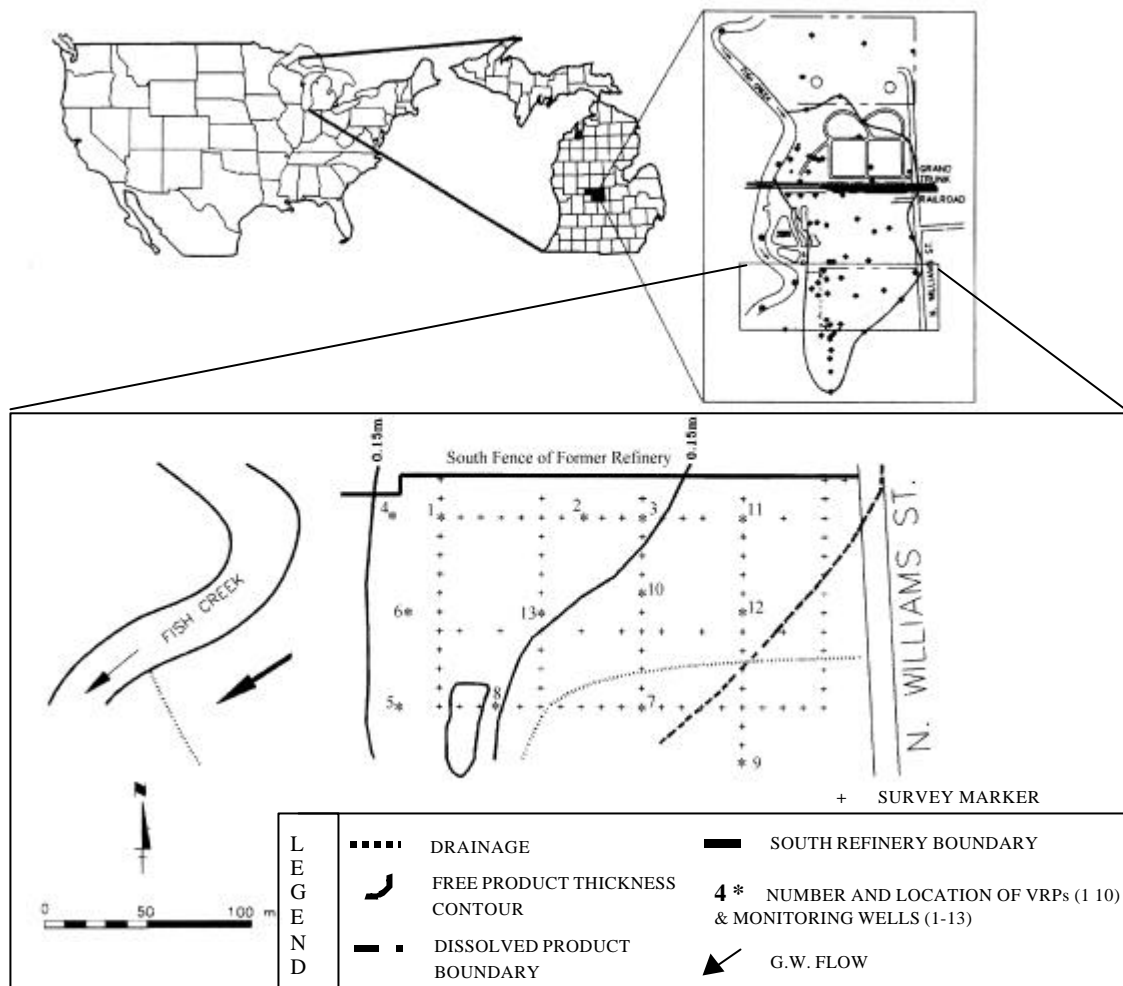


Figure 1. Site location

Study Site

The Crystal Refinery located in Carson City, Michigan (Figure 1) has had historical releases from storage tanks and pipelines resulting in the seepage of hydrocarbons into the subsurface, impacting soils and groundwater beneath the site, cemetery and park, since 1945. Subsequent studies revealed a northern and southern plume originating from the former refinery. This study presents results on investigations focusing on the southern plume extending southwesterly into the City Park. This plume was approximately 750 ft (228.6 m) long and 270 ft (82.3 m) wide with a free product thickness between 1-2 ft (0.31 to 0.61 m) and an estimated volume of 44,000 gallons (167,200 liters) (Snell Environmental Group, 1994). Dissolved phase hydrocarbons are found at the fringes of the free product plume with high concentrations of benzene, toluene, ethyl benzene and xylene (BTEX) (Dell Engineering, 1992).

Geologically, the site is characterized by approximately 15 - 20 ft (4.57 to 6.09 m) of fine to medium sands, coarsening at and below the water table to gravel and is underlain by a 2 - 10 ft (0.61 to 3.05 m) thick clay aquitard unit (Dell Engineering, 1991,1992). Due to topography, the depth to the water table varies from 2 - 3 ft (0.61 m to 0.92 m) west of the site next to Fish Creek to 15 - 19 ft (4.57 to 5.79 m), to the east. Groundwater flows west-southwest toward Fish Creek with a hydraulic gradient of 0.005 ft/ft (0.0015 m/m) and a flow velocity of 5.5 ft/day (1.68 m/day) (Snell Environmental Group, 1994).

Vertical Resistivity Probes

The vertical resistivity probes (VRPs) consist of a 1.5-inch (3.81 cm) ID PVC dry well with ½ inch (1.27 cm) stainless steel screws separated vertically every inch (2.54 cm). The screw heads serve as the electrode contact to the formation and the threaded ends allow contact inside the dry PVC well enabling apparent resistivity readings. Ten vertical resistivity probes are currently installed at the Carson City Park (Figure 1). Installation of these probes includes a small bentonite slurry annulus, which allows installation below the saturated zone and decreases the contact resistance with the surrounding formation sediment.

VRP measurements were made using a Syscal R2 resistivity meter with the automated/semi-automated system developed by Werkema et. al. (1998). Data collection was completed in the semi-automated mode using a mechanical switchbox with a vertical resolution of 2 in. (5.08 cm). Apparent resistivity data were collected using both a 2 in. (5.08 cm) Wenner array and a 4 in. (10.16 cm) pole-dipole array. The data presented in this paper are from the 2 in. (5.08 cm) Wenner array. Data were collected every month for over a period of 12 months or more. Some VRPs were installed earlier in the project and have a larger time span of data. The table below summaries the VRP and time range throughout which monthly measurements were collected.

<i>VRP #</i>	<i>Dates</i>	<i>Days</i>
1	10/19/97 - 11/6/00	1 - 1104
2	2/15/98 - 10/16/00	120 - 1083
3	3/27/99 - 10/16/00	518 - 1083
4	3/20/99 - 10/16/00	511 - 1083
5	4/17/99 - 11/06/00	539 - 1104
6	3/20/99 - 10/16/00	511 - 1083
7	4/17/99 - 10/16/00	539 - 1083
8	3/27/99 - 10/16/00	518 - 1083
9	8/18/99 - 11/06/00	658 - 1104
10	8/18/99 - 11/06/00	658 - 1104

Results

The VRP data are grouped in three categories as follows: free product LNAPL contamination, residual LNAPL contamination, and no contamination (control site). The data are presented with depth indicated as elevation. The water table data is as measured from a 1 in. (2.54 cm) monitoring well located within a 3 foot (91.44 cm) radius from the VRP. Figure 2 presents the water table data versus

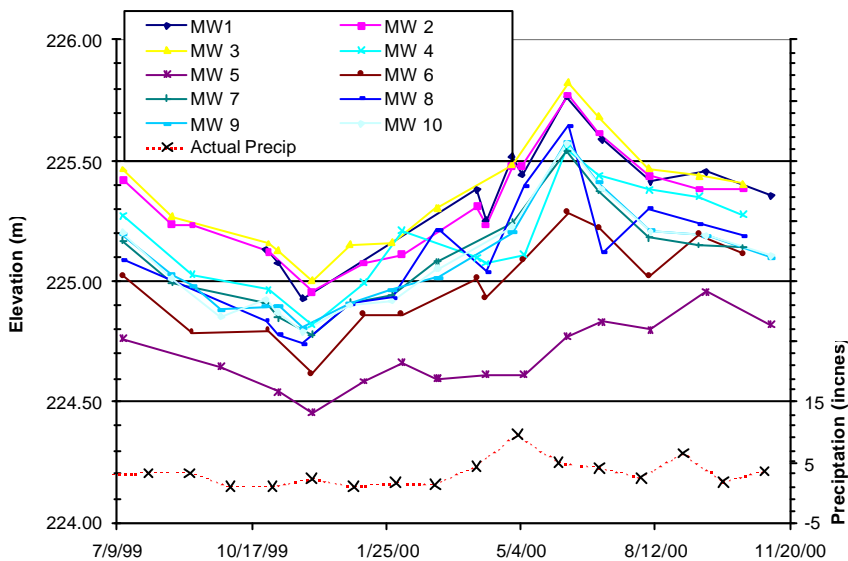


Figure 2. Water table measurements and precipitation versus time

time and precipitation data versus time. The VRP data are presented for each day the reading was taken with the elevation along the vertical axis and the apparent resistivity (Ohm.m) on the horizontal axis.

Free Product LNAPL Contamination

A total of five VRPs are installed in locations where variable levels of free product are observed. Amounts of free product observed range from a few inches to almost 2 feet (60.96 cm). The data from one of these locations, VRP 5 (see Figure 1 for

VRP location), which has one of the largest amounts of free product, are included in Figure 3.

These data are very repeatable and show very little fluctuation over time, with the exception of

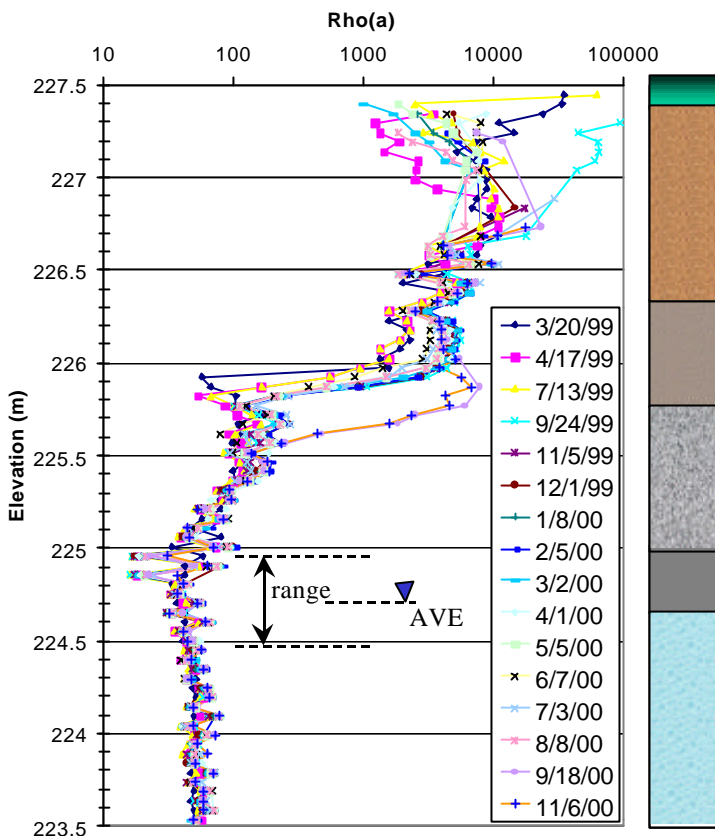


Figure 3. VRP 5, 2'' Wenner, Elevation vs Time. A=Top soil, B=fine-medium tan sand C=moist coarse tan sand, some gravel; D=gray gravel & sand, gasoline odor; E= gray, LNAPL saturated coarse gravel; F=gravelly sand water saturated

of the shallow vadose zone, which is interpreted to reflect soil moisture changes. Noteworthy is the vertical variability over time between 226 meters and 225.5 meters as the geoelectric interface between sediment layer C and D changes. This is interpreted as variations in pore water saturation, as the sediment profile does not change. Other characteristics of the profile indicate the geoelectric response to changes in the soil profile as well as a marked minimum zone occurring below 225 meters and coincident with the upper zone of free product. This area displays a typical Wenner alternating polarity response as the profile continues across the sharp geoelectric boundary between layers D and E (Telford, 1990). Below this zone the profile converges to saturated zone values. Finally, the vadose zone reveals another area of large fluctuations interpreted as vadose zone moisture variations.

Residual LNAPL Contamination

Three VRPs are installed in the residual portion of the LNAPL plume. The data from VRP 3 is included in Figure 4.

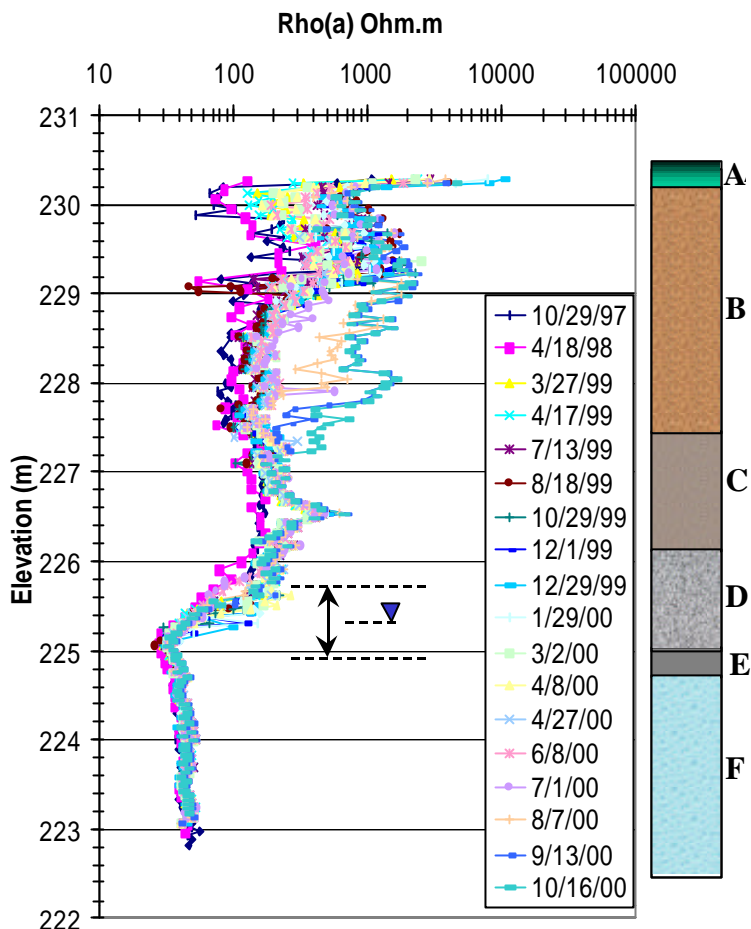


Figure 4. VRP 3, 2'' Wenner, Elevation vs Time. A=Top soil, B=fine-medium tan sand C=moist coarse tan sand, some gravel; D=gray gravel & sand, gasoline odor; E= gray, coarse gravel strong gasoline odor, LNAPL coated grains; F=gravelly sand water saturated

These data continue to show a variable apparent resistivity response in the vadose zone that decreases in variability with depth and corresponds to sediment descriptions A, B and C. The apparent resistivity response decreases abruptly in zone D and continues to a minimum apparent resistivity zone observed at 225.2 meters and corresponding to zone E. Below the saturated zone, the apparent resistivity values show little to no variability. These data reveal a slight VRP response to fluctuating water table levels as observed through small variability or profile shifts from more or less apparent resistivity. Additionally the data shows good correlation with the subsurface geology/stratigraphy. Notably, no alternating polarity response is observed at the water table interface, as in VRP 5, but a zone of minimum apparent resistivity is observed nonetheless and correlates with zone E, a gray coarse gravel with strong gasoline odor. The lack of polarity response suggests that at this location there is no sharp geoelectric boundary as observed at the free product location (VRP 5).

No Contamination (Control Site)

Two VRP locations contain no evidence of LNAPL contamination and are considered the control locations at this site. Figure 5 shows the results from one such location (VRP 9).

The results show some variability in the vadose zone, although not as much as VRPs 5 & 3. The apparent resistivity results show a slight increase above the water table and then a gradual decrease through the transition zone and convergence of the values below the water table and into the saturated zone. These results reveal no resistivity minimum, as observed in VRPs 3 & 5 and a gradual decrease in resistivity through the capillary zone as opposed to the sharp boundary observed in VRP 3 and 5.

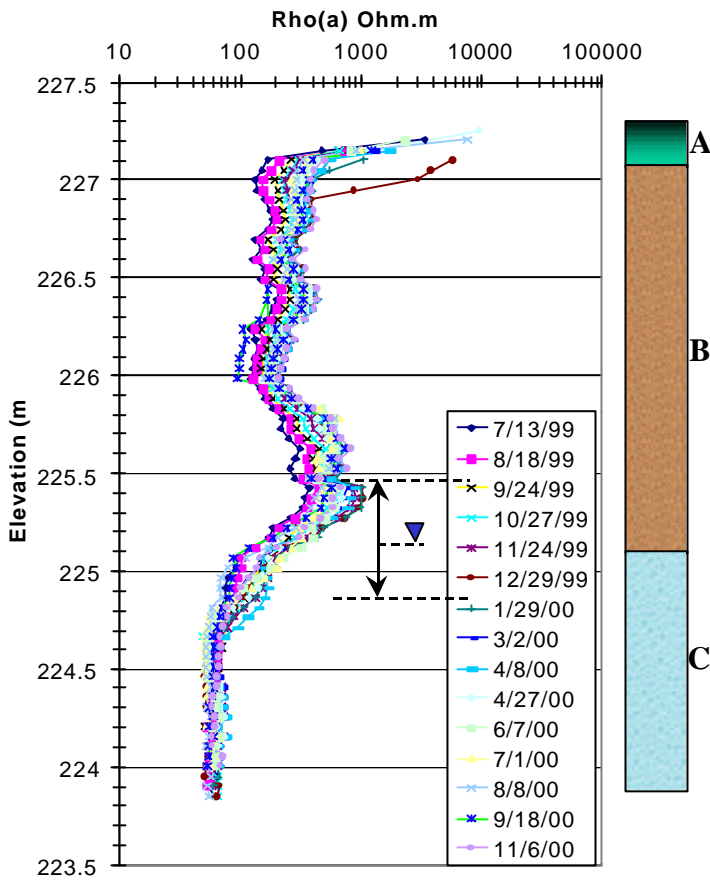


Figure 5. VRP 9, 2'' Wenner, Elevation vs Time. A=Top soil, B=fine-medium tan sand C= gravelly sand water saturated

Additionally, these VRP data reveal changes in the apparent resistivity within the water table fluctuation zone. This variability is probably due to pore water saturation changes over time.

Finally, it is noted that the VRP responds to pore water saturation differently than a monitoring well. That is, the water table data, as determined from the 1" (2.54 cm) monitoring well reveals the top of saturation (Potentiometric surface) whereas the VRP is sensitive to pore water variability and hence, the capillary fringe and transition zone. Furthermore, VRP 9 clearly reveals changes due to fluctuating water levels and/or seasonal precipitation changes, whereas the contaminated locations did not reveal such changes. VRP 5 especially shows very little variability, and VRP 3 only slight changes. This suggests a possible destruction of the natural hydrogeologic profile (i.e. well developed capillary fringe and transition zone) in the contaminated locations versus the clean site (VRP 9) which responds to seasonal hydrogeologic changes.

VRP Depth Zones

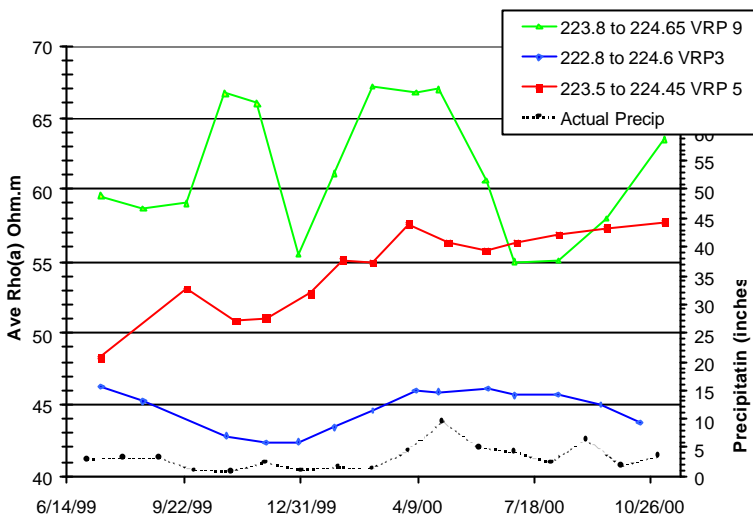


Figure 6. Saturated zone average Rho(a)

VRP average responses from depth zones or depth slices were calculated from the above plots and plotted over time for the analysis of temporal variability. The following plots show these results as well as the actual precipitation values.

Figure 6 shows the saturated zone average apparent resistivity for each VRP. VRPs 3 and 5 reveal a subdued reflection of changes in precipitation during the study time. VRP 9 on the other hand shows large variability over time. This is interpreted as the response of VRP 9 to infiltration events and that the apparent resistivity is free to respond to these events without the influence of LNAPL contamination, as

observed in VRPs 3 and 5. Furthermore, the overall values of average saturated zone apparent resistivity are lower at the LNAPL impacted areas compared to VRP 9, the control site.

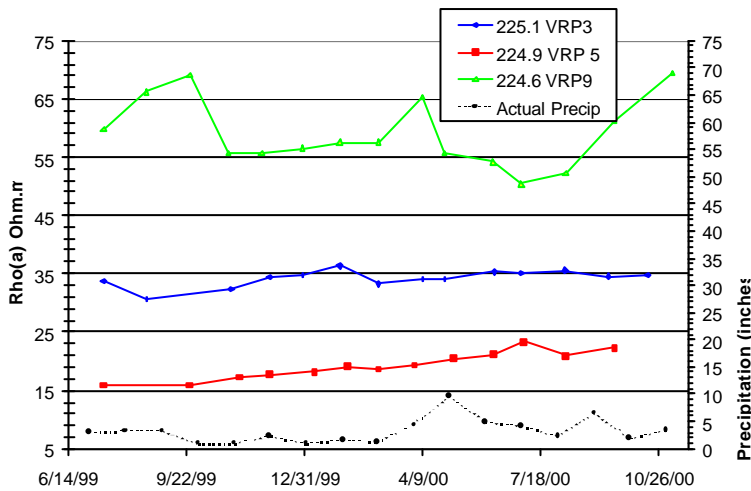


Figure 7. Minimum Rho(a) slice

Figure 7 displays a slice in time from the minimum apparent resistivity zone observed in the apparent resistivity versus elevation plots. These time slices do not exhibit such variability as Figure 6, due to the lack of averaging values. Secondly, VRP 9 again, shows the most variability, which suggests a more representative geoelectric response to natural conditions than the suppressed response from VRPs 3 and 5. Finally, in this minimum apparent resistivity zone, the values indicate that the free product LNAPL site (i.e. VRP 5) results in the lowest apparent resistivity. That is, $VRP\ 5\ r_a < VRP\ 3\ r_a < VRP\ 9\ r_a$.

Figure 8 reveals the average apparent resistivity of the upper transition zone from each VRP represented in this paper. Again, the values show that the more LNAPL contamination the lower the apparent resistivity. VRPs 5 and 3 do show some variability over time and the form of the respective curves appears to emulate the precipitation curve. However, the amplitude of the variability is suppressed due to the scale of the plot and the large variability from VPR 9. This is interpreted, as above, that VRP 9 reveals the non-contaminated natural response to precipitation events. Furthermore, VRP 9 does show a general increase in the apparent resistivity that stabilizes around 12/31/99. This is interpreted as the five-month equilibration of the bentonite slurry, which was used during installation, to the formation.

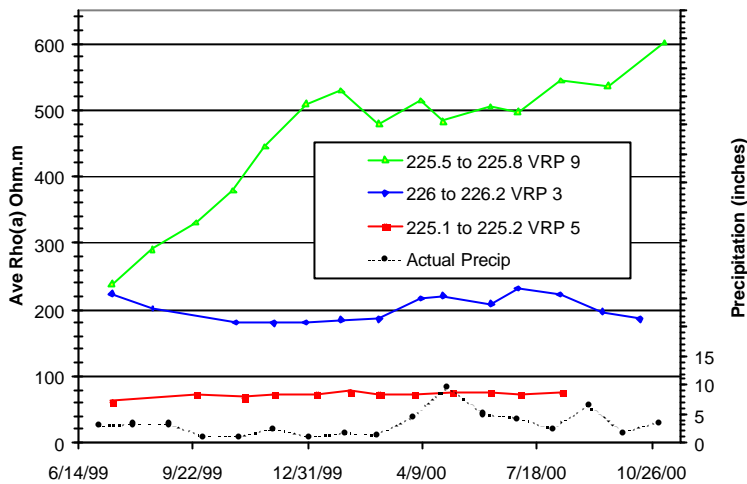


Figure 8. Upper capillary fringe average Rho(a)

Archie's Law Analysis

A detailed comparison between VRPs 3, 5, and 9 is presented from 12-1-99. Figure 9 presents the apparent resistivity versus depth relative to the water table for each of the three VRPs. Positive distance on the vertical axis indicates height above the water table, while negative values are depth below. Evident from this comparison is the gradual decrease in apparent resistivity through the transition zone and stabilizing below the saturated zone for VRP 9. In contrast to this profile are the results for both VRP 3 and VRP 5 which both show a resistivity minimum zone at and above the water table that corresponds to the zone where either an immiscible LNAPL phase and/or dissolved LNAPL are present. In order to illustrate this point the depths from +50 to -40 are shown in an expanded view.

These VRP data are analyzed by making some simple comparative calculations based on Archie's Law (Archie, 1942).

First, we assumed the changes in apparent conductivity above the water table were due completely to variations in water saturation. This approach would be consistent with the insulating layer model for LNAPL pools. The apparent water saturation was estimated for each of the above VRPs. The saturation index (SI) was calculated as a function of depth (z) using.

$$SI(z) = \frac{r_a(z)}{r_{a\text{ ave}}}$$

Where the uncontaminated saturated zone $r_{a\text{ ave}} = 64.7$ ohm.m. Apparent water saturation was determined using $S_w(z) = SI(z)^{-n}$ where it was assumed that $n=2$.

Figure 10 shows the results from these estimations with an expanded view of the zone about the water table. Overall, this figure reveals that to explain the results from VRP 3 and VRP 5 excess water saturation is necessary to account for the lowered apparent resistivity relative to the uncontaminated location, VRP 9. Therefore, according

to the typical insulating layer geoelectrical model for LNAPL impact sites, large water saturation would have to occur to account for the VRP results observed. This result is obviously in conflict with the fact that the LNAPL should be displacing the pore water and lowering water saturation. As a result, another mechanism must be acting in the impacted zone, which is suggested to account for the anomalously lower apparent resistivity. Furthermore, VRP 5 shows the greatest variability, which may suggest differences in permeability, porosity or some heterogeneity responsible for the varied response. Such heterogeneity is suggested to be a result of the large free product layer at the VRP 5 location.

Hence, the question becomes what increase in pore water conductivity is necessary to account for the VRP data. To answer this question, we again used Archie's Law to analyze the anomalous low resistivity responses observed at the LNAPL free product contaminated location (VRP 5) and the LNAPL residual contamination location (VRP 3). It was assumed that the water saturation profile $S_w(z)$ at VRP 5 and VRP 3 are the same as for the uncontaminated section at VRP 9. This approach should give an estimate of the minimum pore water conductivity enhancement. For a given elevation relative to the water table, it can be shown from Archie's Law that the ratio between the pore water resistivities for

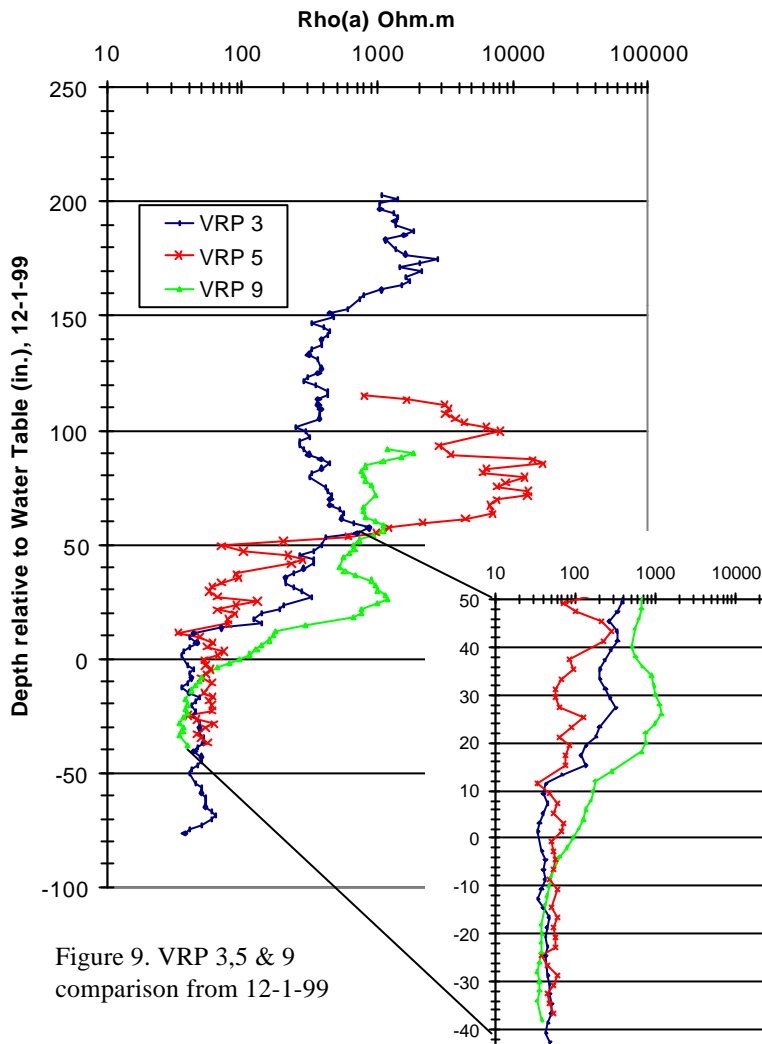


Figure 9. VRP 3,5 & 9 comparison from 12-1-99

the contaminated and uncontaminated sections is equal to the ratio between the apparent resistivities measured, that is

$$\frac{\mathbf{r}^c(z)}{\mathbf{r}^{uc}(z)} = \frac{\mathbf{r}_w^c(z)}{\mathbf{r}_w^{uc}(z)}$$

This ratio was determined for both VRP 3 and 5 using the data from VRP 9 as the uncontaminated profile $\mathbf{r}^{uc}(z)$

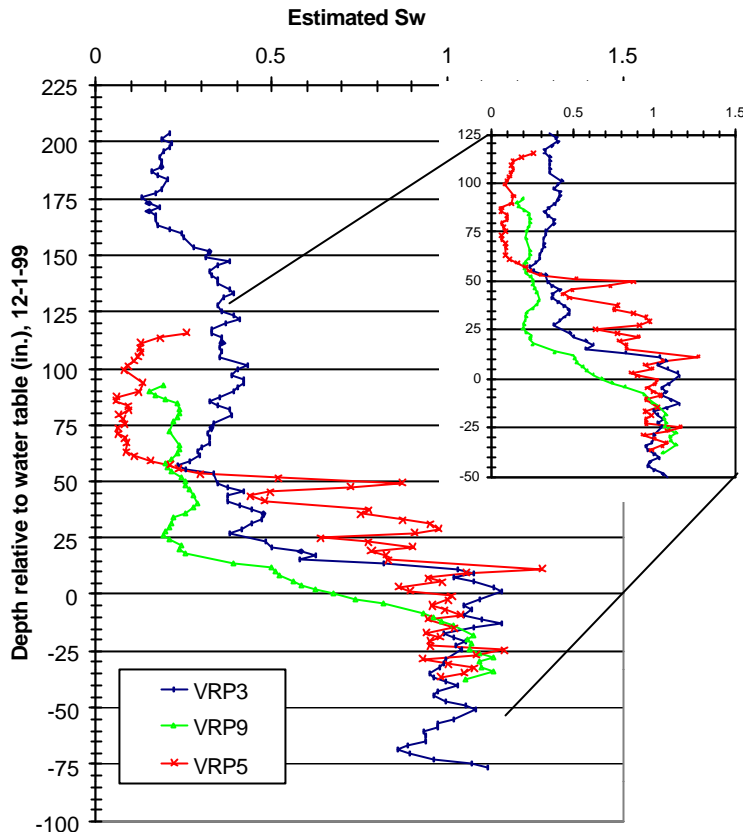


Figure 10. VRP 3,5 & 9, Estimated apparent water saturation (S_w) necessary to account for the changes in apparent resistivity from field measurements, assuming the insulating layer model for LNAPL pools.

The computed pore water ratio profile was then used to determine pore water conductivity profile at the contaminated sites by assuming that the water conductivity at the uncontaminated site has a constant value of 31 mS/m.

The resulting pore water conductivity profiles for the contaminated sites are given in Figure 11. These results show that a very large pore water conductivity enhancement is necessary to account for the VRP results observed at the contaminated locations VRP 3 & 5. In fact, this estimate may be the minimum enhancement value, as water displacement by the LNAPL would further lower S_w at the contaminated sites, requiring a larger pore water conductivity enhancement to account for the field measurements. Therefore, the mechanism of conductivity enhancement due to microbial mediated processes of hydrocarbon degradation may explain the conductivity enhancement necessary. This result is contradictory to the insulating layer model and further supports the anomalous conductivities observed at this site and others in Michigan (Sauck et al., 1998).

Conclusions

The results presented in this paper document over one year of VRP readings at three locations at a site impacted with LNAPL contamination. The VRP resistivity - elevation plots reveal that the natural hydrogeologic regime is not present in LNAPL contaminated areas as fluctuations of the water table are not observed in these VRPs, but evident in the control or non-contaminated VRP. It appears that the oil-water interface remains a mixed zone and the contamination masks or overrides the hydrologic

variations throughout the seasons. Furthermore, the VRPs correlate well with the sediment descriptions. Select VRP depth sections and slices indicate that the apparent resistivity is lowest in the LNAPL free

product locations, progressively higher in the LNAPL dissolved location and highest in the clean (i.e. non-contaminated) location. These VRP sections also respond in like form to precipitation events, however at the contaminated locations the magnitude of change is greatly suppressed due to the contamination. Finally, a simple analysis using Archie's Law reveals that the insulating layer model would require a large water saturation increase at the contaminated site; this result is inconsistent with the expected displacement of water by LNAPL. Another analysis based on Archie's Law shows that a large pore water conductivity enhancement is necessary to produce the VRP field results from contaminated locations. Overall, these results further support that at a site of long term LNAPL contamination with glacially derived sediment, predominately sand and small gravel, the geoelectric response is conductive rather than the traditionally accepted resistive layer. The results presented in this paper give further evidence that VRPs can be a very useful method to understand the hydrogeologic dynamics at a LNAPL contaminated site.

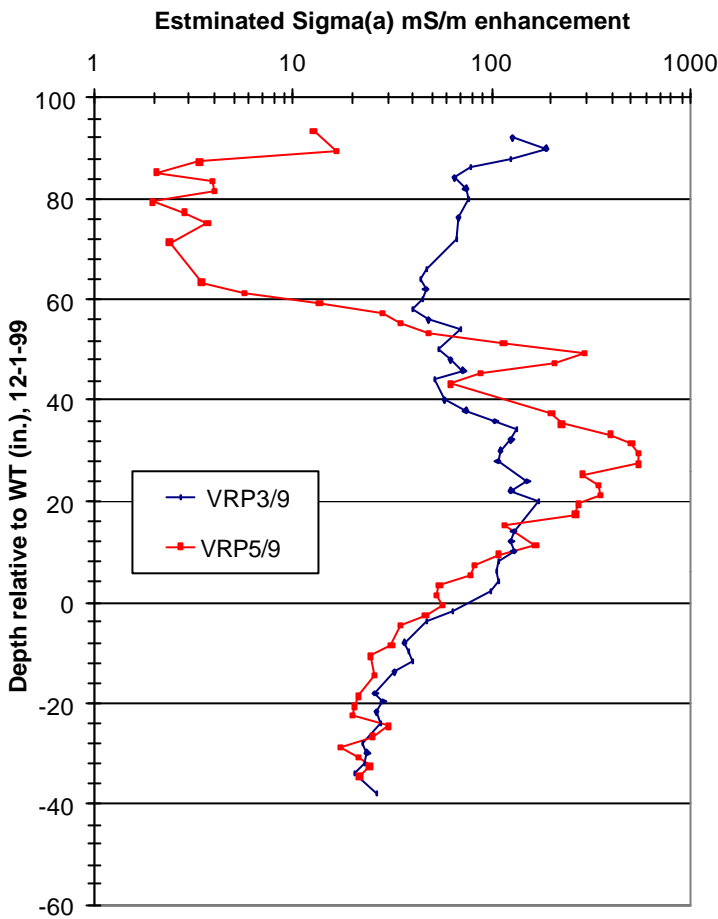


Figure 11. VRP 3,5 & 9, Estimate of the minimum pore water conductivity enhancement necessary to account for the VRP field measurements, assuming the insulating layer model for LNAPL pools.

References

- Archie, G.E., 1942, The Electrical Resistivity Log as an Aid in Determining Some Reservoir Characteristics, Transactions of the American Institute of Mining, Metallurgical and Petroleum Engineers. 146, 54-62.
- Atekwana, E.A., Sauck, W.A., Werkema Jr., D., 2000, Investigations of Geoelectrical Signatures at a Hydrocarbon Contaminated Site, Journal of Applied Geophysics, 44/2-3, 167-180.
- Cassidy, D.P., Werkema, D.D., Sauck, W.A., Atekwana, E.A., Rossbach, S., and Duris, J. 2001, The effects of LNAPL biodegradation products on electrical conductivity measurements, Journal of Environmental and Engineering Geophysics, vol., 6, p. 47-52.
- Dell Engineering, Inc., 1992, Remedial Action Plan for Crystal Refining Company, 801 North Williams Street, Carson City, MI. Report DEI No. 921660, Holland, Michigan.

- De Ryck, S.M., Redman, J.D., and Annan, A.P., 1993, Geophysical Monitoring of a Controlled Kerosene Spill, Proceedings of the Symposium on the Application of Geophysics to Engineering and Environmental Problems (SAGEEP'93), San Diego, CA, 5-20.
- Sauck, W.A., 2000 A Conceptual Model for the Geoelectrical Response of LNAPL Plumes in Granulated Sediments, *Journal of Applied Geophysics* 44/2-3, 151-165
- Sauck, W.A., Atekwana, E.A., and Nash, M.S., 1998, High Conductivities Associated with an LNAPL Plume Imaged by Integrated Geophysical Techniques; *Journal of Environmental and Engineering Geophysics*, Vol. 2, No. 3, 203-212.
- Snell Environmental Group, Inc., 1994, Technical Memorandum Task 1B - IRAP Evaluation, Crystal Refinery, 801 N. Williams Street, Carson City, Michigan, MERA ID #59003.
- Telford, W.M., Geldart, L.P., and Sheriff, R.E., 1990, *Applied Geophysics* Second Edition, Cambridge University Press, 558.
- Werkema Jr., D.D., Atekwana A., Sauck, W., Rossbach S., and Duris, Vertical Distribution of Microbial Abundances and Apparent Resistivity at an LNAPL Spill Site D. SAGEEP 2000 pp..
- Werkema Jr., D.D. Atekwana, E.A., Sauck, W.A., Asumadu, J., 1998, A Versatile Windows Based Multi-Electrode Acquisition System for DC Electrical Methods Surveys, *Environmental Geosciences*, Vol. 5, No. 4, 196-206.